European Journal of Radiology 145 (2021) 110013

Contents lists available at ScienceDirect

European Journal of Radiology

journal homepage: www.elsevier.com/locate/ejrad

Kidney tumor diffusion-weighted magnetic resonance imaging derived ADC histogram parameters combined with patient characteristics and tumor volume to discriminate oncocytoma from renal cell carcinoma

Tim J. van Oostenbrugge [a,*,1], Ilse M. Spenkelink [b,1], Louisa Bokacheva [c], Henry Rusinek [d], Martin J. van Amerongen [b], Johan F. Langenhuijsen [a], Peter F.A. Mulders [a], Jurgen J. Fütterer [b]

[a] Department of Urology Radboud University Medical Center, Nijmegen, the Netherlands
[b] Department of Radiology and Nuclear Medicine Radboud University Medical Center, Nijmegen, the Netherlands
[c] Department of Radiology, New York University School of Medicine, New York, NY, USA
[d] Center for Advanced Imaging Innovation and Research (CAI2R) and Department of Radiology, New York University School of Medicine, New York, NY, USA

ARTICLE INFO

Keywords:
Renal cell carcinoma
Kidney neoplasms
Oncocytoma
Magnetic resonance imaging
Diffusion weighted MRI

ABSTRACT

Purpose: To assess the ability to discriminate oncocytoma from RCC based on a model using whole tumor ADC histogram parameters with additional use of tumor volume and patient characteristics.
Method: In this prospective study, 39 patients (mean age 65 years, range 28–79; 9/39 (23%) female) with 39 renal tumors (32/39 (82%) RCC and 7/39 (18%) oncocytoma) underwent multiparametric MRI between November 2014 and June 2018. Two regions of interest (ROIs) were drawn to cover both the entire tumor volume and a part of healthy renal cortex. ROI ADC maps were calculated using a mono-exponential model and ADC histogram distribution parameters were calculated. A logistic regression model was created using ADC histogram parameters, radiographic and patient characteristics that were significantly different between oncocytoma and RCC. A ROC curve of the model was constructed and the AUC, sensitivity and specificity were calculated. Furthermore, differences in intra-patient ADC histogram parameters between renal tumor and healthy cortex were calculated. A separate ROC curve was constructed to differentiate oncocytoma from RCC using statistically significant intra-patient parameter differences.
Results: ADC standard deviation ($p = 0.008$), entropy ($p = 0.010$), tumor volume ($p = 0.012$), and patient sex ($p = 0.018$) were significantly different between RCC and oncocytoma. The regression model of these parameters combined had an ROC-AUC of 0.91 with a sensitivity of 86% and specificity of 84%. Intra-patient difference in ADC 25th percentile ($p < 0.01$) and entropy ($p = 0.030$) combined had a ROC-AUC of 0.86 with a sensitivity and specificity of 86%, and 81%, respectively.
Conclusion: A model combining ADC standard deviation and entropy with tumor volume and patient sex has the highest diagnostic value for discrimination of oncocytoma. Although less accurate, intra-patient difference in ADC 25th percentile and entropy between renal tumor and healthy cortex can also be used. Although the results of this preliminary study do not yet justify clinical use of the model, it does stimulate further research using whole tumor ADC histogram parameters.

1. Introduction

Renal cell carcinoma (RCC) comprises 85% of all renal cancers. With more than 400,000 new cases worldwide in 2018, RCC is considered the seventh most common malignancy in the developed world [1].

The majority of renal lesions suspected for RCC are incidental findings on imaging performed for reasons other than diagnosis of RCC [2]. Contrast enhanced CT and MRI are used to differentiate lesions

Abbreviations: ADC, Apparent Diffusion Coefficient; AUC, Area Under the Curve; BMI, Body Mass Index; DWI, Diffusion Weighted Imaging; RCC, Renal Cell Carcinoma; ROC, Receiver Operator Characteristics; ROI, Region of Interest.

* Corresponding author at: Radboud University Medical Center, Department of Radiology, P.O. Box 9101, 6500 HB Nijmegen, The Netherlands.
E-mail address: tim.vanoostenbrugge@radboudumc.nl (T.J. van Oostenbrugge).

[1] Shared first authorship.

https://doi.org/10.1016/j.ejrad.2021.110013
Received 20 September 2021; Received in revised form 20 October 2021; Accepted 26 October 2021
Available online 30 October 2021

suspicious for malignancy within this group of renal tumors [3,4]. Despite their routine use, these imaging techniques cannot completely reliably distinguish RCC from several benign renal tumors, specifically oncocytoma [5,6]. The best sensitivity to predict the presence of a renal oncocytoma on multiphasic contrast enhanced CT scan has been found for a homogenous enhancement of a renal tumor and is 81% [7].

This lack in ability to discriminate is due to the appearance of oncocytoma as solitary, well demarcated, hypervascular, contrast enhancing renal cortical tumors on imaging, which mimics the appearance of RCC [8]. Renal tumor biopsy may be helpful, but oncocytoma are often difficult to distinguish from chromophobe RCC, and up to one-third of the oncocytic tumors are hybrid and have a malignant component [9,10]. In recent studies of partial nephrectomy, about 20% of all resected lesions suspected for RCC are shown to be benign, with the majority of these lesions being oncocytoma [11,12].

In patients with localized RCC and treated with curative intent, the 5-year recurrence rates range from 20 to 30% [13]. There is an extremely wide range of 5-year survival rate ranging from 9 to 81% depending on TNM stage, nuclear grade and RCC subtype. In a recent study of 1015 patients with metastatic RCC (stage IV) a median survival of only 8.7 months was observed for 641 patients who received targeted therapy and 7.2 months for nontargeted therapy [14]. On the other hand, oncocytomas have no malignant potential, and only sporadically show renal vein invasion, and local recurrence after surgery [15,16]. Therefore, active surveillance is considered a proper management alternative for histologically proven oncocytomas, especially in case of smaller tumors [4,17]. Thus, superfluous surgery and invasive diagnostics, such as renal biopsies, can be avoided if oncocytomas can be discriminated noninvasively from RCC on imaging.

Diffusion-weighted imaging has proven to be a promising diagnostic imaging modality for genitourinary malignancies [18]. In renal tumors, apparent diffusion coefficient (ADC) values are lower for RCC compared to oncocytoma [19]. Several recent studies used the mean ADC value obtained from small regions of interest (ROIs) within the tumor for differentiation of renal tumors [20]. However, this method is susceptible to variability in ROI placement which is an inherent limitation. Also, placement of smaller ROIs may not reflect all histopathologic features in the tumor [21]. Literature shows overlap in mean RCC and non-RCC ADC values using this method, hampering use of ADC values in clinical practice [19]. To develop a clinically applicable model, the predictive measure should be measured quickly and reliably, i.e. independent of ROI placement. Recent studies suggest the use of whole tumor ADC distribution parameters, such as entropy, skewness, and kurtosis for differentiation of small renal masses [21,22]. Apart from DWI parameters, predictors for renal tumor malignancy are tumor size and male sex [23]. We hypothesized that a composite classification model that includes DWI-derived measures, such as ADC distribution parameters, tumor volume *and* demographic characteristics may reliably distinguish RCC from oncocytoma.

The purpose of this study was to assess the ability to discriminate oncocytoma from RCC based on the ADC distribution parameters with additional use of tumor volume, and patient demographic characteristics.

2. Materials and methods

2.1. Patients

This prospective study, performed at the Radboud University Medical Center, was compliant with Health Insurance Portability and Accountability Act, approved by local institutional review board and registered on clinicaltrials.gov (NCT02325921). Written informed consent was obtained from each eligible patient before enrollment.

Because whole tumor volume ADC histogram parameters were unavailable at the time the study was initiated, a difference in mean ADC values considered relevant for the study endpoint was formulated on basis of relevant literature, and used for sample size calculation. The formula used for sample size calculation is: $N = 2(Z\alpha + Z\beta)^2 * s^2/d^2$. α was set at 0.05 (two sided test) and β was set at 0.10. Corresponding $Z\alpha$ and $Z\beta$ were 1.96, and 1.28, respectively. "s" was the expected standard deviation which was set at 0.3 s/mm^2, "d" was the considered relevant difference in mean ADC values between histological subtype of renal tumors which was set at 0.5 s/mm^2 [5,24]. Using this formula and ADC values, approximately 7 patients should be evaluated in every group. Because oncocytoma was expected to be the smallest group, the study was ended when 7 oncocytoma evaluable on study endpoint were included.

Between October 2014 and June 2018, a total of 45 consecutive patients planned to undergo (partial) nephrectomy and 3 for a renal tumor biopsy were included in the study. Inclusion criteria were: radiologic diagnosis of renal tumor based on previous ultrasonography, CT or MRI examinations; being at least 18 years of age; and histopathologically confirmed renal tumor diagnosis. Exclusion criteria were: contraindications for MRI (non-MR compatible metal device/foreign bodies, claustrophobia); an active renal or *peri*-renal infection; prior treatment for renal malignancies; cystic tumor; artefacts in DWI images impeding accurate tumor segmentation and reliable parameter calculation, and known metastatic disease.

Data of 9 patients who underwent surgery were excluded for the following reasons: severe imaging artifacts within the tumor (n = 2); presurgical tumor embolization (n = 1); cystic tumors (n = 3); or absence of histologically confirmed renal tumor (n = 3). The final cohort included 39 patients (9 females, mean age 65 years, range: 38–79) with 39 lesions (3 biopsy proven): 32 malignant RCCs (25 clear cell, 2 chromophobe, 3 papillary, 1 clear cell papillary, and 1 mucinous tubular and spindle cell RCC), and 7 oncocytomas (Table 1).

Table 1
Patient demographics and tumor characteristics.

Variable	Renal cell carcinoma (n = 32)	Oncocytoma (n = 7)
Age (y)	65.1 (38–79)	64.7 (28–75)
No. of women	5 (16)	4 (57)
Body mass index (kg/m^2)	27.8 (22.0–36.7)	26.9 (20.7–35.2)
Tumor volume (cm^3)	262.4 (5.7–1261.1)	47.9 (3.5–169.2)
Affected side		
Left	16 (50.0)	2 (28.6)
Right	16 (50.0)	5 (71.4)
Type of procedure		
Robot assisted laparoscopic partial nephrectomy	7 (21.9)	4 (57.1)
Open partial nephrectomy	1 (3.1)	0
Laparoscopic radical nephrectomy	9 (28.1)	0
Open radical nephrectomy	15 (46.9)	0
Percutaneous biopsy	0	3 (42.9)
Tumor stage		
T1	14 (43.8)	6 (85.7)
T2	1 (3.1)	1 (14.3)
T3	16 (50)	0
T4	1 (3.1)	0
Histological subtype RCC		N/A
Clear cell	25 (78.1)	
Papillary	3 (9.4)	
Chromophobe	2 (6.3)	
Papillary clear cell	1 (3.1)	
Mucinous tubular and spindle cell	1 (3.1)	
Nuclear grading (Fuhrman)		N/A
I	1 (3.1)	
II	10 (31.3)	
III	11 (34.4)	
IV	7 (21.9)	
Unknown	3 (9.4)	

Note: Data are presented as mean (range) or No. (%). RCC = renal cell carcinoma, N/A = not applicable.

Patients' renal medical history, as well as the information about diagnoses, biopsies, and surgical procedures were collected. Pre-operative chronic kidney disease (CKD) stage based on serum creatinine level was assessed according to standard clinical practice [25]. Demographic data, including age, sex and body mass index (BMI), were also collected [23].

2.2. Imaging protocol

Imaging was performed within 21 days prior to surgery or biopsy using a 3T MRI system (Magnetom Trio, Siemens Healthineers, Erlangen, Germany) and a combination of a 32-channel receiver coil and phased array body surface coil. Patients were positioned in a feet-first supine position. The scanning protocol included breath hold anatomical T2-weighted multi-slice half-Fourier-acquired single-shot turbo spin echo (HASTE) sequences in axial and coronal directions. DWI was performed using a respiratory triggered coronal single-shot-echo-planar imaging (SS-EPI) sequence with b-values of 50, 800 and 1400 s/mm^2 with diffusion gradients applied in three orthogonal directions (see Table 2 for detailed parameters).

2.3. Image analysis

The image analysis workflow is shown in Fig. 1. DICOM images were exported to an offline work-station for processing. Respiratory motion artifacts in DW images with different b-values were minimized by one reader (IS) using semi-automatic co-registration (FireVoxel, CAI^{2}R, New York University, NY). Registration was done separately for each kidney (with and without the tumor), resulting in two datasets for each patient. Next, two observers blinded for clinical and histopathological information (IS and MA, with 1 and 3 years of experience in abdominal imaging, respectively), independently drew ROIs on both registered DWI datasets. Both readers were supervised by a radiologist (JF, 15 years of experience in abdominal radiology). In tumor-bearing kidneys, the ROI covered the entire tumor on all slices where tumor was visible. ROIs were also drawn in the contralateral kidneys covering at least 5 cm^3 of the cortex for reference measurements. The volumes of the ROIs were calculated. To reduce partial volume effects, edge voxels were removed from the ROI using a 3D morphological erosion [26]. A mono-exponential model, $S_b/S_0 = \exp(-b \bullet ADC)$, was fitted voxel-wise to the measured signal intensities (S_b), where b is the diffusion sensitivity parameter and $S_0 = S(b = 0)$, using a nonlinear least squares method in MATLAB (v. R2019a, MathWorks; Natick; MA, USA). The voxel-based ADC values of the tumor and renal cortex ROIs were then used for histogram analysis.

Voxels with extreme signal intensity values (outside Tukey's fences with k = 1.5 based on the histogram analysis) were considered not representative. To avoid influence of the resulting extreme ADC values on the histogram analysis those voxels were removed from the analysis [27]. Then, the following ADC histogram parameters were derived: mean, mode, standard deviation, 5th percentile, 10th percentile, 25th percentile, 75th percentile, 95th percentile, entropy, skewness and kurtosis. (Fig. 2). Inter-observer agreement for tumor volume and histogram parameters were tested in ten randomly selected cases.

Table 2
Magnetic resonance imaging parameters.

Imaging parameter	T2WI Axial	T2WI Coronal	DWI
TR/TE (ms)	2000/92	2000/103	2800/77
Flip angle ()	150	140	90
No. of slices	30	30	35
Slice thickness (mm)	4	5	4
Field of view (mm)	450 × 450	400 × 400	380 × 309
Matrix size	320 × 256	320 × 256	192 × 154
Voxel size (mm × mm)	1.4 × 1.8	1.3 × 1.6	2.0 × 2.5
b-values (s/mm^2)	N/A	N/A	50/800/1400

Note: T2WI = T2-weighted magnetic resonance imaging, DWI = diffusion weighted magnetic resonance imaging, TR = repetition time; TE = echo time, N/A = not applicable.

2.4. Pathological assessment

Biopsy or surgical pathology specimens obtained from solid tumor regions were fixed in formalin, embedded in paraffin, cut into 4-μm sections and stained with hematoxylin and eosin. Histopathological diagnoses were made by a board-certified pathologist, according to WHO classification of renal tumors [28].

2.5. Statistical analysis

For descriptive analysis, median (range) and mean (±SD) values were calculated. Interobserver agreement, including 95% confidence intervals, between tumor volumes and histogram measures of ten randomly selected cases obtained by the two readers was tested using an intraclass correlation coefficient (ICC, absolute agreement). The ICC greater than 0.70 and 0.80 were interpreted as a good and excellent agreement, respectively.

The Mann-Whitney test was used to compare the ADC histogram parameters between the RCCs and oncocytomas and to compare the tumor volume, age and BMI in the two patient groups. The differences between the two groups by patient sex were assessed using the Chi-square test.

To discriminate oncocytoma from RCC, a logistic regression model was created using parameters that were significantly different between the two tumor types or patient groups. Collinearity of model parameters was tested using the variance inflation factor (VIF), defined as $VIF = 1/(1 - R^2)$, where R^2 is the coefficient of determination between a given predictor (parameter) and all other predictors. A VIF > 4 was considered as presence of multicollinearity, and such parameters were excluded from the model.

First, logistic regression analysis for predicting oncocytoma was performed using only the imaging derived parameters. A second model was constructed by adding the demographic parameters. Receiver Operating Characteristic (ROC) curves for both regression models were created and the area under the curve (AUC) was calculated. The optimal sensitivity and specificity were selected by maximizing the Youden's index (J = sensitivity + specificity-1). The ROC curves were compared using the DeLong method [29]. Standard errors (SE) and confidence intervals (CI) of AUC were calculated for comparison of the models (www.medcalc.org).

A subgroup analysis including only oncocytoma and clear cell RCCs was performed using logistic regression for predicting oncocytoma presence. Likewise to the previous models, first, a model only including the significantly different imaging derived parameters was constructed followed by a second model including significantly different patient characteristics.

A separate analysis was performed to evaluate the discriminative value for oncocytoma using intra-patient ADC histogram parameter differences between renal tumor and healthy renal cortical tissue. The ADC histogram parameter differences in the oncocytoma and RCC group were compared using the Mann-Whitney test. ADC histogram parameters with significant, non-collinear differences between the oncocytoma and RCC groups were used for logistic regression analysis to predict oncocytoma and an ROC-AUC was calculated for this regression model. To better translate findings to clinic, rather than consensus measurement, measures from one observer (IS) were used for predictive modeling.

Analyses were done using Statistical Package for the Social Sciences version 25.0 (SPSS, IBM, Armonk, New York, USA). For all tests a p-value ≤ 0.05 was considered statistically significant.

3. Results

Mean tumor volumes measured by reader IS and MA were 237 cm^3

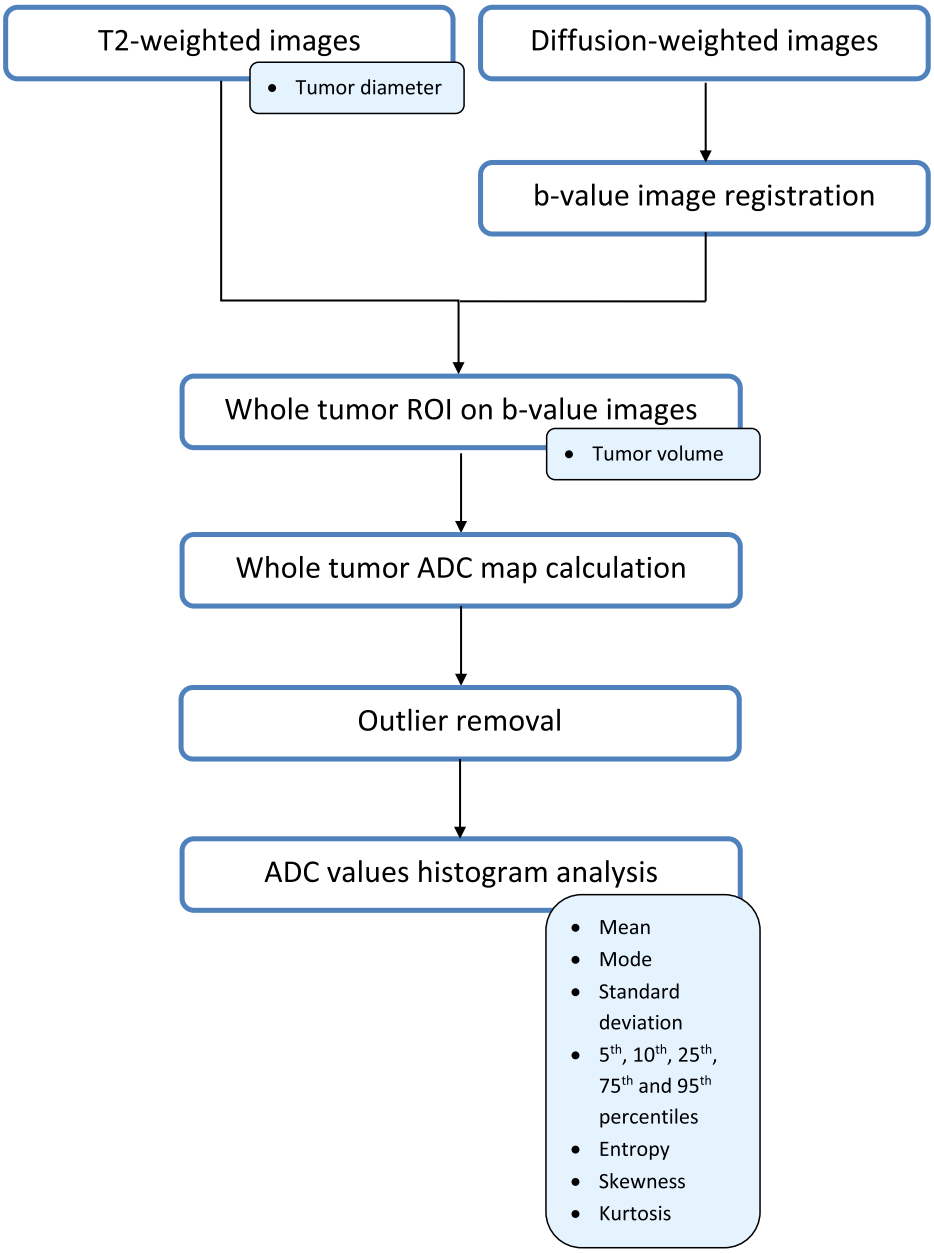

Fig. 1. Image analysis workflow.

(range, 11–604 cm^3) and 222 cm^3 (range, 11–538 cm^3), respectively. The interobserver agreement for tumor volume was excellent (ICC, 0.98). For the ADC histogram parameters, agreement was as follows: mode 0.60, entropy 0.72, skewness 0.78, kurtosis 0.81; and for SD, mean and all percentiles 0.98–0.99. Therefore, analyses were done using the ROIs drawn by reader IS.

3.1. Imaging derived parameters

The ADC standard deviation and ADC entropy were statistically significantly different between oncocytoma and RCC. The ROC-AUC for these two parameters separately were 0.17 and 0.81, respectively. The ADC mean, mode, kurtosis, and the ADC percentiles did not differ significantly between the two tumor types (Table 3).

Mean largest tumor diameter was 7.6 ± 3.2 cm (range, 2.2–14.6 cm) for RCC and 4.2 ± 2.1 cm (range, 2.2–7.1 cm) for oncocytoma. The mean tumor volumes differed significantly between RCC (262 ± 291 cm^3; range, 6–1261 cm^3) and oncocytoma (48 ± 59 cm^3; range, 3–169 cm^3). The ROC-AUC for tumor volume was 0.19.

No multicollinearity between the significantly different imaging derived parameters was present. Therefore, three imaging-derived parameters - ADC standard deviation, ADC entropy, and tumor volume - were used in the regression models. The imaging derived parameter regression model ROC-AUC was 0.90, with the maximum sensitivity and specificity of 86% and 81%, respectively (Fig. 3).

3.2. Incremental use of demographics

Analysis of demographic parameters showed sex to be statistically significantly different between RCC and oncocytoma patients. Patient age and BMI were not significantly different between the two groups (Table 3). No multicollinearity between the significant ADC histogram parameters and sex was observed. ROC-AUC for sex was 0.71. The addition of patient sex to the imaging derived parameter regression model resulted in ROC-AUC of 0.93 (AUC difference 0.03; 95% C.I. −0.033 to 0.087; SE. 0.03) (Fig. 3). The maximum sensitivity and

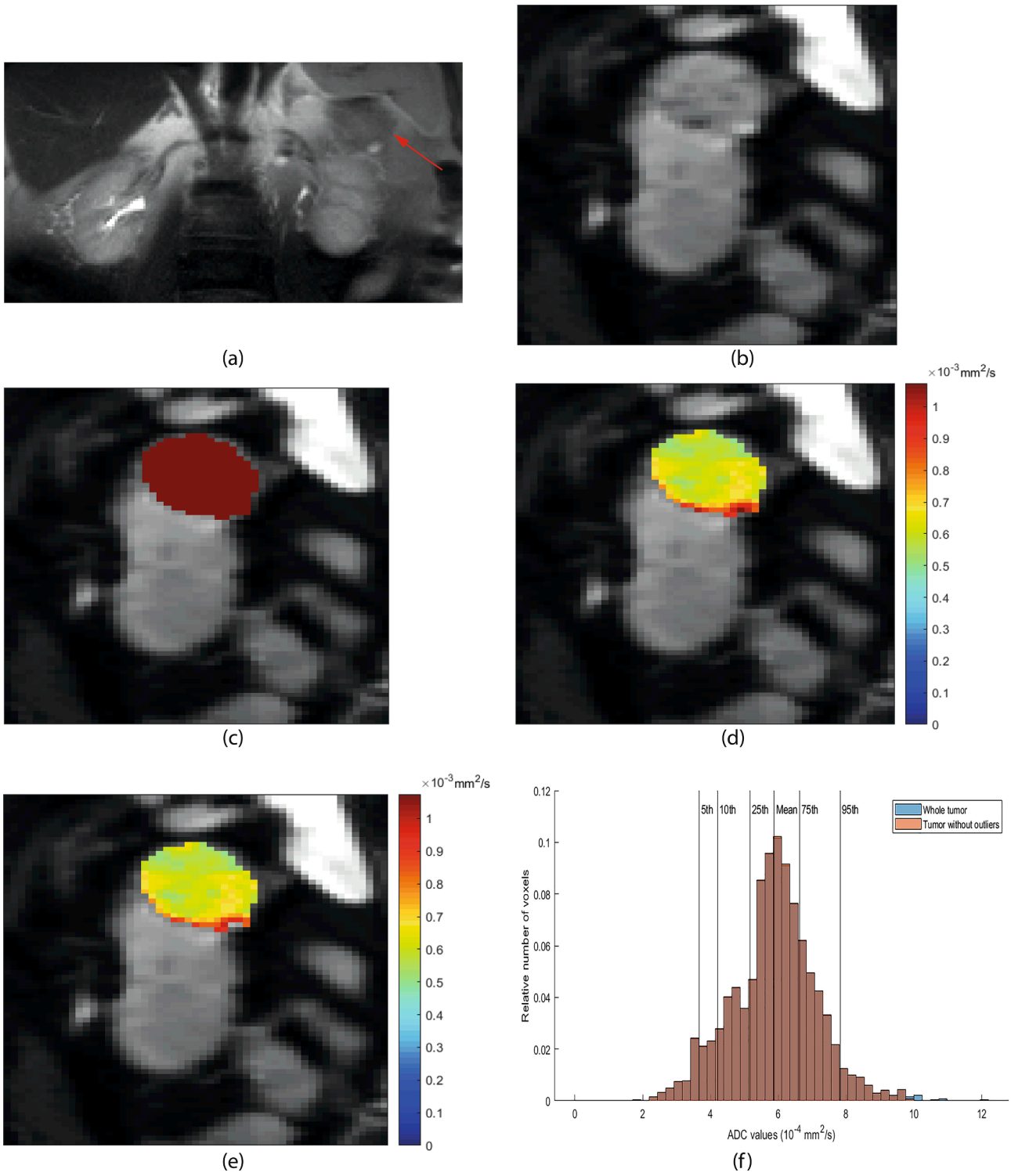

Fig. 2. Coronal T2-weighted image, showing a tumor (oncocytoma, red arrow) in the left kidney (A). Coronal diffusion weighted image (b = 50 mm^2/s) showing the same oncocytoma (B). Region of interest at one of the slices is shown in red (C). Calculated ADC map of the region of interest (D). ADC map of region of interest after outlier removal (based on volumetric ADC histogram) (E). In (D-E), color bars show ADC values in s/mm^2. In (F) the histogram of ADC values in this tumor is shown. Whole tumor ADC values after outlier removal are shown in red. The outliers are depicted in blue. The vertical lines represent the mean and percentiles used for statistical analysis.

specificity were 86% and 84%, respectively.

3.3. Oncocytoma versus clear cell RCC sub analysis

For the DWI histogram parameters in the subgroup analysis only the ADC standard deviation and ADC entropy were statistically significantly different between oncocytoma and clear cell RCC, likewise to the analysis including all RCC subtypes. The ADC mean, mode, kurtosis, and the ADC percentiles didn't differ between the two tumor types (Table 4). The ROC-AUC for these two parameters separately were 0.09 and 0.82

Table 3
Demographic and apparent diffusion coefficient histogram parameters in the renal cell carcinoma and oncocytoma groups.

Variable	Renal Cell Carcinoma (n = 32)	Oncocytoma (n = 7)	*p*-value*
Sex			0.018**
Men	27 (84)	3 (43)	
Women	5 (16)	4 (57)	
Age (y)	65.1 ± 9.2	64.7 ± 16.6	0.359
BMI (kg/m^2)	27.8 ± 3.8	26.9 ± 5.0	0.583
Tumor volume (cm^3)	262 ± 291	48 ± 59	0.012
Tumor diameter (cm)	7.6 ± 3.2	4.2 ± 2.1	0.013
Histogram parameters			
Mean	1.50 ± 0.32	1.49 ± 0.59	0.770
Mode	1.35 ± 0.31	1.48 ± 0.59	0.400
Standard deviation	0.40 ± 0.15	0.22 ± 0.09	0.008
Skewness	0.33 ± 0.31	0.08 ± 0.42	0.133
Kurtosis	−0.05 ± 0.54	0.07 ± 0.41	0.464
Entropy	3.14 ± 0.14	3.31 ± 0.15	0.010
5th percentile	0.90 ± 0.30	1.13 ± 0.51	0.200
10th percentile	1.01 ± 0.28	1.20 ± 0.52	0.242
25th percentile	1.21 ± 0.28	1.34 ± 0.55	0.380
75th percentile	1.77 ± 0.41	1.63 ± 0.64	0.826
95th percentile	2.22 ± 0.50	1.89 ± 0.71	0.242

Note: Data are mean ± standard deviation; data in parentheses are percentages. Mean, mode, standard deviation, and percentiles of apparent diffusion histogram parameters are in $\times 10^{-3}$ mm^2/s.

* Group differences were tested with the Mann-Whitney test, unless stated otherwise.

** Group difference tested with the chi-square test.

respectively. Furthermore, the median tumor volume differed significantly between clear cell RCC and oncocytoma (151 cm^3; range, 6–1261 cm^3 versus 41 cm^3; range, 3–169 cm3). The ROC-AUC for tumor volume was 0.14.

In the absence of any multicollinearity between the significantly different imaging derived parameters - ADC standard deviation, ADC entropy, and tumor volume - were used in this subanalysis likewise to the previous regression models including all RCC subtypes. The ROC-AUC of the imaging derived parameter regression model was 0.94, with the maximum sensitivity and specificity of 88% and 86%, respectively. Sex was the only statistically significantly different demographic parameter between clear cell RCC and oncocytoma patients with an ROC-AUC of 0.71. The addition of patient sex to the imaging derived parameter regression model resulted in ROC-AUC of 0.94 (AUC difference 0.03; 95% C.I. −0.033 to 0.087; SE. 0.03) (Fig. 4). The maximum sensitivity and specificity for this model were 84% and 100%, respectively.

3.4. Intra-patient ADC histogram differences

Intra-patient comparison of ADC histogram parameter difference between healthy renal cortex and tumor tissue showed a significant

Table 4
Demographic and apparent diffusion coefficient histogram parameters in the clear cell renal cell carcinoma and oncocytoma groups.

Variable	Renal Cell Carcinoma (n = 25)	Oncocytoma (n = 7)	*p*-value*
Sex			0.035**
Men	21 (84)	3 (43)	
Women	4 (16)	4 (57)	
Age (y)	66.4 ± 8.6	64.7 ± 16.6	0.537
BMI (kg/m^2)	27.9 ± 3.8	26.9 ± 5.0	0.632
Tumor volume (cm^3)	303.0 ± 310.9	48 ± 59	0.004
Tumor diameter (cm)	8.1 ± 3.3	4.2 ± 2.1	0.006
Histogram parameters			
Mean	1.57 ± 0.30	1.49 ± 0.59	0.982
Mode	1.40 ± 0.28	1.48 ± 0.59	0.538
Standard deviation	0.43 ± 0.13	0.22 ± 0.09	0.001
Skewness	0.28 ± 0.28	0.08 ± 0.42	0.245
Kurtosis	−0.15 ± 0.48	0.07 ± 0.41	0.245
Entropy	3.13 ± 0.16	3.31 ± 0.15	0.011
5th percentile	0.92 ± 0.30	1.13 ± 0.51	0.264
10th percentile	1.05 ± 0.28	1.20 ± 0.52	0.327
25th percentile	1.27 ± 0.27	1.34 ± 0.55	0.509
75th percentile	1.87 ± 0.37	1.63 ± 0.64	0.538
95th percentile	2.34 ± 0.44	1.89 ± 0.71	0.096

Note: Data are mean ± standard deviation; data in parentheses are percentages. Mean, mode, standard deviation, and percentiles of apparent diffusion histogram parameters are in $\times 10^{-3}$ mm^2/s.

* Group differences were tested with the Mann-Whitney test, unless stated otherwise.

** Group difference tested with the chi-square test.

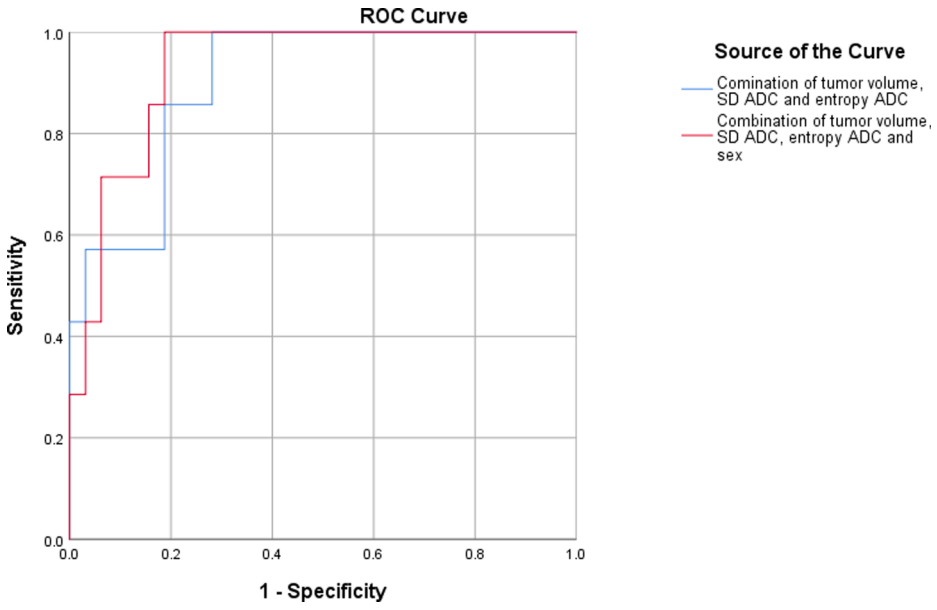

Fig. 3. Receiver operator characteristic curves of the logistic regression models to predict oncocytoma presence. Depicted in blue is the ROC curve combining the imaging-derived parameters: tumor volume, ADC standard deviation, and entropy. Depicted in red is the ROC curve for the model with incremental use of sex. AUC for the imaging alone is 0.91, for the combined model this is 0.93.

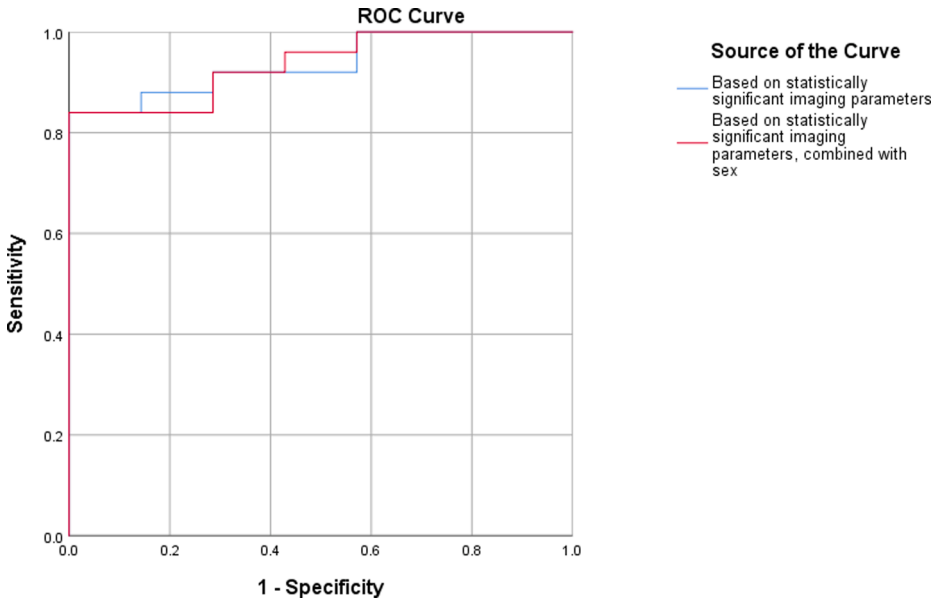

Fig. 4. Receiver operator characteristic curves of the subgroup analysis including only clear cell RCC with logistic regression models to predict oncocytoma presence. Depicted in blue is the ROC curve combining the imaging-derived parameters: tumor volume, ADC standard deviation, and entropy. Depicted in red is the ROC curve for the model with incremental use of sex. AUC for the imaging alone is 0.94, for the combined model this is 0.94 as well.

difference in mean ADC, entropy and 5th, 10th, and 25th percentile between RCC and oncocytoma (Table 5). Because multicollinearity was found for mean ADC and ADC percentiles, only the 25th percentile was used in the regression model combined with entropy because it has the highest individual sensitivity (86%) and specificity (88%). ROC-AUC for the model combining ADC entropy and 25th percentile was 0.86 with a maximum sensitivity and specificity of 86%, and 81%, respectively.

4. Discussion

In this study we show that renal whole tumor ADC distribution parameters are of value in discriminating oncocytoma from RCC. A model combining these parameters with tumor volume and patient sex yields the highest diagnostic value to predict the presence of an oncocytoma.

Direct comparison of renal tumor mean ADC values between different studies is cumbersome. Studies including the analysis of oncocytoma are very scarce and numbers do not exceed 16 cases per study [30]. In recent literature 13 studies analyzed ADC values collected from a total of 69 oncocytoma, resulting in an ADC value ranging between 1.61 and 2.40 mm^2/s [19,31,32]. In agreement with our findings, mean oncocytoma ADC values reported in literature overlap with RCC ADC values. Accordingly, it is not feasible to derive reliable thresholds for ADC values [31].

Several factors may contribute to the reported heterogeneity in ADC values. First, differences in the used equipment and imaging parameters are a major issue. Studies evaluating the optimal imaging parameters are lacking, resulting in a wide variety of used protocols hampering direct comparison of results between different studies. Second, most reported studies used subjective free hand placement of ROIs covering small parts of the tumor for obtaining ADC values. Voxel signal intensity heterogeneity within the tumor, based on histopathologic features, makes this approach prone to inter-/intraobserver variability. Third, the use of mean ADC values for tumor characterization is susceptible to extreme ADC values within a tumor.

To avoid subjective ROI placement and potential sampling bias, and to reduce the effect of ADC value heterogeneity on our analysis, we used whole tumor volume analysis. This method resulted in a good inter-observer agreement. However, accurate whole tumor segmentation and subsequent ADC parameter calculation requires high quality images with minimum artefacts. In daily practice these images may be hard to acquire because of - for instance - movements of the kidney due to breathing. In our study two scans were excluded from analysis due to artifacts hampering accurate tumor segmentation. This may introduce a bias in favor of the diagnostic accuracy of the model. Furthermore, to reduce the effect of extreme ADC values in the differentiation of renal tumors, diffusion parameter histogram analysis can be of value because distribution parameters are independent of signal intensity [33].

We showed that tumor ADC standard deviation and entropy have discriminative value for predicting benign nature of renal tumors. Our findings are in concordance with the study by Li et al., analyzing whole tumor volumes of 92 renal masses <4 cm, including 7 oncocytoma and 13 angiomyolipoma [34]. Their study showed a significant difference in entropy between oncocytoma and the three most common RCC subtypes. Also, a significant difference in ADC standard deviation value between papillary RCC and oncocytoma was found. Histogram analysis failed to show significant differences in ADC mean, median, and percentiles, as well as in skewness and kurtosis. In the study by Li et al. the highest AUC (0.851; optimal 80%; specificity 86%) for differentiating malignant from all benign renal tumors combined was achieved in a

Table 5
Intra-patient apparent diffusion coefficient histogram parameter differences between renal tumor and healthy cortex.

Variable	Renal Cell Carcinoma	Oncocytoma	*p*-value *
Tumor volume (cm^3)	262 ± 291	48 ± 59	0.012
Healthy cortex volume (cm^3)	11.5 ± 3.2	11.5 ± 2.4	1.000
Mean	−2.76 ± 0.55	−2.13 ± 0.71	0.030
Mode	−2.75 ± 0.55	−1.91 ± 1.23	0.050
Standard deviation	−0.09 ± 0.18	−0.16 ± 0.15	0.310
Skewness	0.32 ± 0.51	0.28 ± 0.59	0.770
Kurtosis	−0.39 ± 0.62	0.0.30 ± 0.41	0.630
Entropy	−0.07 ± 0.19	0.10 ± 0.14	0.030
5th percentile	−2.55 ± 0.62	−1.82 ± 0.76	0.010
10th percentile	−2.63 ± 0.56	−1.90 ± 0.76	0.010
25th percentile	−2.74 ± 0.52	−2.04 ± 0.72	<0.010
75th percentile	−2.79 ± 0.61	−2.24 ± 0.74	0.060
95th percentile	−2.86 ± 0.74	−2.36 ± 0.71	0.090

Note: Data are in mean ± standard deviation. Mean, mode, standard deviation, and percentiles are in $\times 10^{-3}$ mm^2/s.

* Group differences were tested with the Mann-Whitney test.

model combining ADC mean, 90th percentile, and entropy. ADC histogram parameters cannot be compared directly to our study due to differences in imaging parameters. Also, AUCs in our study are not provided for differentiation of oncocytoma separately. In contrast to our study, Paschall et al. concluded that clear cell RCC cannot be differentiated from oncocytoma using whole volume ADC histogram parameters based on their study including 26 oncocytoma, 97 clear cell, and 29 papillary RCCs. Analysis of ADC histogram parameters (including median, mean, skewness, kurtosis and a wide variety of percentiles) of papillary versus clear cell RCC and papillary RCC versus oncocytoma did show significant differences. In their study also larger and complex cystic tumors were included, and for diffusion-weighted imaging b-values with a maximum of 800 s/mm^2 were used.

We also analyzed the predictive value of non-diffusion weighted radiographic and demographic features. In agreement with a study by Bhindi et al., we found that smaller tumor size (although our study used volume instead of largest diameter) and female gender are predictive for a benign tumor [35]. Their study only included T1-2 tumors (300 benign, and 2350 malignant). The number of included oncocytomas is not clear. Although other studies reported differences in age or patient BMI between RCC and oncocytoma, we did not confirm these findings. Our finding is supported by a recent meta-analysis analyzing composite models and nomograms including radiographic results combined with demographic or clinical characteristics. This analysis, including 20 studies with 12.149 patients, showed that the only significant predictors of malignancy were tumor size (effect size, 1.33-fold increased risk per centimeter), and male sex (effect size, 2.71). The results were not significant for other tumor characteristics, age, and BMI [23]. Despite being in line with existing literature, results from our study regarding patient sex should be interpreted with care due to the uneven distribution of men and women between the RCC and oncocytoma groups. The smaller sample size of our cohort is the most likely explanation for the strong male predominance in the RCC group, which does not reflect the 2:1 male predominance from larger studies [1]. This uneven distribution may skew result in favor of women having an oncocytoma, and the true impact of adding patient sex to a composite model may be less significant.

Oncocytoma and chromophobe RCC share morphologic, immunohistochemical, molecular, and ultrastructural characteristics. These similar characteristics make it hard to histologically distinguish oncocytoma from especially the eosinophilic variant of chromophobe RCC [9]. This specific differentiation is stressed by the malignant potential of chromophobe RCC lacking in oncocytoma. Furthermore, 3% - in case of solitary small renal tumors - up to one-third - mostly in the context of genetic disorders - of the oncocytic tumors are hybrid and have a RCC, thus malignant, component [10,36]. This can be a potential pitfall for renal mass biopsies. A previous study analyzing MRI features (DWI not included) of oncocytoma and chromophobe RCC showed overlap in imaging parameters and concluded that differentiation was not reliably possible [5]. Unfortunately, our study did not include enough chromophobe RCC cases for a separate analysis.

Using whole tumor analysis on imaging, selective tumor (under) sampling is avoided and small foci of RCC in hybrid tumors may be diagnosed. This may have a significant impact on the choice of treatment. The insight on the natural course of untreated renal tumors has grown due to an increase in patients followed by active surveillance. The risk for progression differs between the histological subtypes of RCC, with clear cell RCC being an unfavorable subtype [37]. Thus, an increased ability to characterize renal lesion through imaging may lead to a change in clinical decision making.

The generalizability of our method to a different dataset is important for future development of prediction models to aid clinical decision making. The predictive value of sex and tumor size has been confirmed in multiple studies. However, the direct comparability of diffusion parameters to other studies, such as mean ADC value, is depending heavily on the used imaging parameters. The use of histogram distribution parameters, such as entropy, is not dependent on signal intensity and may be a more robust parameter for comparison between studies. Future studies including larger, and most likely more heterogeneous datasets for analysis using machine learning techniques may benefit from the use of these parameters.

This study has several other limitations. Due to the small numbers, the included RCC subtypes (clear cell, papillary and chromophobe) were grouped for analysis. The unique tissue characteristics of these subtypes may have contributed to a broader range in parameter values. However, the subanalysis in which these subtypes were excluded did not alter our findings. Focus of future studies should be differentiation of oncocytoma from especially clear cell and chromophobe RCC, as papillary RCC can often be differentiated based on the enhancement pattern. Larger cohorts better reflecting real world data should be used to confirm our findings. Another possible drawback for use in clinical routine may be the methods used for image analysis in this study, which are software dependent and time consuming. Also, clinical decision making is not only dependent on the odds of a renal lesion being malignant. Other factors such as comorbidities and tumor characteristics increasing the risk for surgical complications should be taken into account. Models taking these factors into account are very complicated to develop.

In conclusion, we showed that renal whole tumor ADC distribution parameters are of value in discriminating oncocytoma from RCC. A model combining ADC standard deviation and entropy, tumor volume, and patient sex yielded the highest diagnostic value. Intra-patient difference in ADC 25th percentile and entropy between renal tumor and healthy cortex can also be of additional value. Although the diagnostic accuracy of the proposed model, and the preliminary data on which the results are based do not yet justify clinical use, this study does stimulate further research using whole tumor ADC histogram parameters to differentiate renal tumors.

CRediT authorship contribution statement

Tim J. van Oostenbrugge: Conceptualization, Methodology, Software, Validation, Formal analysis, Investigation, Resources, Data curation, Writing – original draft, Visualization, Project administration. **Ilse M. Spenkelink:** Conceptualization, Methodology, Software, Validation, Formal analysis, Investigation, Data curation, Writing – original draft, Visualization. **Louisa Bokacheva:** Methodology, Software, Formal analysis, Writing – review & editing. **Henry Rusinek:** Conceptualization, Methodology, Software, Writing – review & editing, Supervision. **Martin J. van Amerongen:** Formal analysis, Investigation, Writing – review & editing. **Johan F. Langenhuijsen:** Writing – review & editing. **Peter F.A. Mulders:** Conceptualization, Writing – review & editing, Supervision. **Jurgen J. Fütterer:** Conceptualization, Writing – review & editing, Supervision.

Declaration of Competing Interest

The authors declare that they have no known competing financial interests or personal relationships that could have appeared to influence the work reported in this paper.

Acknowledgements

The authors would like to thank Nicole Wake for her contribution to initial drafts of the manuscript.

References

[1] F. Bray, J. Ferlay, I. Soerjomataram, R.L. Siegel, L.A. Torre, A. Jemal, Global cancer statistics 2018: GLOBOCAN estimates of incidence and mortality worldwide for 36 cancers in 185 countries, CA Cancer J. Clin. 68 (6) (2018) 394–424.

[2] G. Novara, V. Ficarra, A. Antonelli, W. Artibani, R. Bertini, M. Carini, S. Cosciani Cunico, C. Imbimbo, N. Longo, G. Martignoni, G. Martorana, A. Minervini, V. Mirone, F. Montorsi, R. Schiavina, C. Simeone, S. Serni, A. Simonato,

S. Siracusano, A. Volpe, G. Carmignani, Validation of the 2009 TNM version in a large multi-institutional cohort of patients treated for renal cell carcinoma: are further improvements needed? Eur. Urol. 58 (4) (2010) 588–595.
[3] G.M. Israel, M.A. Bosniak, How I do it: Evaluating renal masses, Radiology 236 (2) (2005) 441–450.
[4] B. Ljungberg, K. Bensalah, S. Canfield, S. Dabestani, F. Hofmann, M. Hora, M. A. Kuczyk, T. Lam, L. Marconi, A.S. Merseburger, P. Mulders, T. Powles, M. Staehler, A. Volpe, A. Bex, EAU guidelines on renal cell carcinoma: 2014 update, Eur. Urol. 67 (5) (2015) 913–924.
[5] A.B. Rosenkrantz, N. Hindman, E.F. Fitzgerald, B.E. Niver, J. Melamed, J.S. Babb, MRI features of renal oncocytoma and chromophobe renal cell carcinoma, AJR Am. J. Roentgenol. 195 (6) (2010) W421–W427.
[6] S. Choudhary, A. Rajesh, N.J. Mayer, K.A. Mulcahy, A. Haroon, Renal oncocytoma: CT features cannot reliably distinguish oncocytoma from other renal neoplasms, Clin. Radiol. 64 (5) (2009) 517–522.
[7] A. Heidenreich, V. Ravery, European Society of Oncological U. Preoperative imaging in renal cell cancer, World J. Urol. 22 (5) (2004) 307–315.
[8] S.R. Prasad, V.R. Surabhi, C.O. Menias, A.A. Raut, K.N. Chintapalli, Benign renal neoplasms in adults: cross-sectional imaging findings, AJR Am. J. Roentgenol. 190 (1) (2008) 158–164.
[9] N.A. Abrahams, P. Tamboli, Oncocytic renal neoplasms: diagnostic considerations, Clin. Lab. Med. 25 (2) (2005) 317–339.
[10] S. Ginzburg, R. Uzzo, T. Al-Saleem, E. Dulaimi, J. Walton, A. Corcoran, E. Plimack, R. Mehrazin, J. Tomaszewski, R. Viterbo, D.Y.T. Chen, R. Greenberg, M. Smaldone, A. Kutikov, Coexisting hybrid malignancy in a solitary sporadic solid benign renal mass: implications for treating patients following renal biopsy, J. Urol. 191 (2) (2014) 296–300.
[11] M. Remzi, E. Javadli, M. Özsoy, Management of small renal masses: a review, World J. Urol. 28 (3) (2010) 275–281.
[12] M. Remzi, M. Özsoy, H.-C. Klingler, M. Susani, M. Waldert, C. Seitz, J. Schmidbauer, M. Marberger, Are small renal tumors harmless? Analysis of histopathological features according to tumors 4 cm or less in diameter, J. Urol. 176 (3) (2006) 896–899.
[13] S. Dabestani, C. Beisland, G.D. Stewart, K. Bensalah, E. Gudmundsson, T.B. Lam, W. Gietzmann, P. Zakikhani, L. Marconi, S. Fernandéz-Pello, S. Monagas, S. P. Williams, C. Torbrand, T. Powles, E. Van Werkhoven, R. Meijer, A. Volpe, M. Staehler, B. Ljungberg, A. Bex, Long-term Outcomes of Follow-up for Initially Localised Clear Cell Renal Cell Carcinoma: RECUR Database Analysis. *Eur Urol Focus* 5 (5) (2019) 857–866.
[14] P. Li, J. Jahnke, A.R. Pettit, Y.N. Wong, J.A. Doshi, Comparative Survival Associated With Use of Targeted vs Nontargeted Therapy in Medicare Patients With Metastatic Renal Cell Carcinoma (vol 2, e195806, 2019), Jama Network Open 2 (2019).
[15] G. Kovacs, M. Akhtar, B.J. Beckwith, P. Bugert, C.S. Cooper, B. Delahunt, J.N. Eble, S. Fleming, B. Ljungberg, L.J. Medeiros, H. Moch, V.E. Reuter, E. Ritz, G. Roos, D. Schmidt, J.R. Srigley, S. Störkel, E. Van Den Berg, B. Zbar, The Heidelberg classification of renal cell tumours, J. Pathol. 183 (2) (1997) 131–133.
[16] B. Perez-Ordonez, G. Hamed, S. Campbell, R.A. Erlandson, P. Russo, P.B. Gaudin, et al., Renal oncocytoma: a clinicopathologic study of 70 cases, Am. J. Surg. Pathol. 21 (1997) 871–883.
[17] S. Kawaguchi, K.A. Fernandes, A. Finelli, M. Robinette, N. Fleshner, M.A.S. Jewett, Most renal oncocytomas appear to grow: observations of tumor kinetics with active surveillance, J. Urol. 186 (4) (2011) 1218–1222.
[18] A. Diaz de Leon, D. Costa, I. Pedrosa, Role of Multiparametric MR Imaging in Malignancies of the Urogenital Tract, Magn. Reson. Imaging Clin. N. Am. 24 (1) (2016) 187–204.
[19] E.A. Lassel, R. Rao, C. Schwenke, S.O. Schoenberg, H.J. Michaely, Diffusion-weighted imaging of focal renal lesions: a meta-analysis, Eur. Radiol. 24 (1) (2014) 241–249.
[20] A.Q. Li, W. Xing, H.J. Li, Y. Hu, D.Y. Hu, Z. Li, et al., Subtype Differentiation of Small (<= 4 cm) Solid Renal Mass Using Volumetric Histogram Analysis of DWI at 3-T MRI, Am. J. Roentgenol. 211 (2018) 614–623.
[21] A.M. Hötker, Y. Mazaheri, A. Wibmer, J. Zheng, C.S. Moskowitz, S.K. Tickoo, P. Russo, H. Hricak, O. Akin, Use of DWI in the Differentiation of Renal Cortical Tumors, Am. J. Roentgenol. 206 (1) (2016) 100–105.
[22] H. Chandarana, A.B. Rosenkrantz, T.C. Mussi, S. Kim, A.A. Ahmad, S.D. Raj, J. McMenamy, J. Melamed, J.S. Babb, B. Kiefer, A.P. Kiraly, Histogram analysis of whole-lesion enhancement in differentiating clear cell from papillary subtype of renal cell cancer, Radiology 265 (3) (2012) 790–798.
[23] P.M. Pierorazio, H.D. Patel, M.H. Johnson, S.M. Sozio, R. Sharma, E. Iyoha, E. B. Bass, M.E. Allaf, Distinguishing malignant and benign renal masses with composite models and nomograms: A systematic review and meta-analysis of clinically localized renal masses suspicious for malignancy, Cancer 122 (21) (2016) 3267–3276.
[24] B. Taouli, R.K. Thakur, L. Mannelli, J.S. Babb, S. Kim, E.M. Hecht, V.S. Lee, G. M. Israel, Renal lesions: characterization with diffusion-weighted imaging versus contrast-enhanced MR imaging, Radiology 251 (2) (2009) 398–407.
[25] KDIGO Clinical Practice Guideline for the Evaluation and Management of Chronic Kidney Disease, Kidney Int. Suppl. 3 (2013) 1–150.
[26] R.W.R. Gonzalez, Morphological Image Processing, in: Digital Image Processing, second ed., Addison-Wesley Publishing Company, Boston, MA, 1992, pp. 525–528.
[27] R. Brant, Comparing Classical and Resistant Outlier Rules, J. Am. Stat. Assoc. 85 (412) (1990) 1083–1090.
[28] H. Moch, A.L. Cubilla, P.A. Humphrey, V.E. Reuter, T.M. Ulbright, The 2016 WHO Classification of Tumours of the Urinary System and Male Genital Organs-Part A: Renal, Penile, and Testicular Tumours, Eur. Urol. 70 (1) (2016) 93–105.
[29] E.R. DeLong, D.M. DeLong, D.L. Clarke-Pearson, Comparing the areas under two or more correlated receiver operating characteristic curves: a nonparametric approach, Biometrics 44 (3) (1988) 837, https://doi.org/10.2307/2531595.
[30] F. Cornelis, E. Tricaud, A.S. Lasserre, F. Petitpierre, J.C. Bernhard, Y. Le Bras, M. Yacoub, M. Bouzgarrou, A. Ravaud, N. Grenier, Routinely performed multiparametric magnetic resonance imaging helps to differentiate common subtypes of renal tumours, Eur. Radiol. 24 (5) (2014) 1068–1080.
[31] Y. Li, Y.e. Wang, J. Qin, J. Wu, X. Dai, J. Xu, Meta-analysis of diffusion-weighted imaging in the differential diagnosis of renal lesions, Clin. Imaging 52 (2018) 264–272.
[32] Y. Mytsyk, I. Dutka, B. Yuriy, I. Maksymovych, M. Caprnda, K. Gazdikova, L. Rodrigo, P. Kruzliak, P. Illjuk, A.A. Farooqi, Differential diagnosis of the small renal masses: role of the apparent diffusion coefficient of the diffusion-weighted MRI, Int. Urol. Nephrol. 50 (2) (2018) 197–204.
[33] A.D. de Leon, P. Kapur, I. Pedrosa, Radiomics in Kidney Cancer: MR Imaging, Magn. Reson. Imaging Clin. N. Am. 27 (1) (2019) 1–13.
[34] A. Li, W. Xing, H. Li, Y. Hu, D. Hu, Z. Li, et al., Subtype Differentiation of Small (</= 4 cm) Solid Renal Mass Using Volumetric Histogram Analysis of DWI at 3-T MRI, AJR Am. J. Roentgenol. 211 (2018) 614–623.
[35] B. Bhindi, R.H. Thompson, C.M. Lohse, R.J. Mason, I. Frank, B.A. Costello, A. M. Potretzke, R.P. Hartman, T.A. Potretzke, S.A. Boorjian, J.C. Cheville, B. C. Leibovich, The Probability of Aggressive Versus Indolent Histology Based on Renal Tumor Size: Implications for Surveillance and Treatment, Eur. Urol. 74 (4) (2018) 489–497.
[36] B. Shuch, A. Amin, A.J. Armstrong, J.N. Eble, V. Ficarra, A. Lopez-Beltran, G. Martignoni, B.I. Rini, A. Kutikov, Understanding pathologic variants of renal cell carcinoma: distilling therapeutic opportunities from biologic complexity, Eur. Urol. 67 (1) (2015) 85–97.
[37] K. McAlpine, A. Finelli, Natural history of untreated kidney cancer, World J. Urol. 39 (8) (2021) 2825–2829.